SUBMITTED: 2012 MARCH 14; ACCEPTED: 2012 SEPTEMBER 26
Preprint typeset using LaTeX style emulateapj v. 5/2/11

GIANT GALAXIES, DWARFS, AND DEBRIS SURVEY. I. DWARF GALAXIES AND TIDAL FEATURES AROUND NGC 7331

JOHANNES LUDWIG, ANNA PASQUALI, EVA K. GREBEL
Astronomisches Rechen-Institut, Zentrum für Astronomie der Universität Heidelberg, Mönchhofstr. 12–14, D-69120 Heidelberg, Germany

AND

JOHN S. GALLAGHER III
Department of Astronomy, University of Wisconsin, 475 North Charter Street, Madison, WI 53706-1582, USA
submitted: 2012 March 14; accepted: 2012 September 26

ABSTRACT

The Giant GAlaxies, Dwarfs, and Debris Survey concentrates on the nearby universe to study how galaxies have interacted in groups of different morphology, density, and richness. In these groups we select the dominant spiral galaxy and search its surroundings for dwarf galaxies and tidal interactions. This paper presents the first results from deep wide-field imaging of NGC 7331, where we detect only four low luminosity candidate dwarf companions and a stellar stream that may be evidence of a past tidal interaction. The dwarf galaxy candidates have surface brightnesses of $\mu_r \approx 23$–25 mag arcsec^{-2} with $(g-r)_0$ colors of 0.57–0.75 mag in the Sloan Digital Sky Survey filter system, consistent with their being dwarf spheroidal galaxies (dSph). A faint stellar stream structure on the western edge of NGC 7331 has $\mu_g \approx 27$ mag arcsec^{-2} and a relatively blue color of $(g-r)_0 = 0.15$ mag. If it is tidal debris, then this stream could have formed from a rare type of interaction between NGC 7331 and a dwarf irregular or transition-type dwarf galaxy. We compare the structure and local environments of NGC 7331 to those of other nearby giant spirals in small galaxy groups. NGC 7331 has a much lower ($\sim$2%) stellar mass in the form of early-type satellites than found for M31 and lacks the presence of nearby companions like luminous dwarf elliptical galaxies or the Magellanic Clouds. However, our detection of a few dSph candidates suggests that it is not deficient in low-luminosity satellites.

Subject headings: galaxies: dwarf galaxies: evolution galaxies: formation galaxies: groups: individual: NGC 7331, galaxies: interactions, galaxies: structure

1. INTRODUCTION

Current models of galaxy formation and evolution suggest that the main process of mass assembly is hierarchical growth via minor and major mergers (e.g., White & Frenk 1991). Observationally this hierarchical structure formation can be traced by the characteristic large-scale galaxy distribution of clusters of galaxies as the most luminous and massive concentrations of matter. Most of the luminous mass, however, is not located in these high-density knots of the cosmic web, but instead along its numerous filaments in less massive galaxy groups. In fact, about 85% of the nearby galaxies are not found in galaxy clusters, but are located instead in galaxy groups and in the field (Tully 1987; Karachentsev 2005). Eke et al. (2005) found that the fraction of mass in stars increases with decreasing group size, with Local-Group-sized galaxy agglomerations containing most of the stellar mass.

There are many indications that mergers played a role in forming groups. For instance, the clustering strength increases with group luminosity (Padilla et al. 2004). Within the groups themselves the earlier-type galaxies are more strongly clustered and are usually located closer to the group center (Girardi et al. 2003), mimicking the morphology-density relation of galaxy clusters (e.g., Oemler 1974; Dressler 1980). Dwarf galaxies and satellites also exhibit a morphology-distance and morphology-density relation with respect to their location within groups (e.g., Einasto et al. 1974; van den Bergh 1994; Grebel 1997). Galaxy groups range from poor to rich groups and from apparently little evolved diffuse "clouds" to compact groups with past or ongoing major mergers. This range of types allows us to explore galaxy evolution and environmental effects in groups of different density, and to compare their properties and evolutionary state with those of galaxies in the field or in galaxy clusters (Grebel 2007). The evolutionary end stage may be represented by the so-called fossil groups that contain a dominant, large elliptical galaxy in their center, likely the result of mergers (Jones et al. 2003; D'Onghia et al. 2005).

The best-studied group of galaxies is obviously the Local Group. Its two dominant spiral galaxies, the Milky Way (MW) and M31, are surrounded by a large number of mainly early-type dwarfs, many of which were only detected in recent years (e.g., Zucker et al. 2004, 2006, 2007; Belokurov et al. 2006, 2007; Martin et al. 2009; Richardson et al. 2011). The vast majority of the Local Group dwarfs are dwarf spheroidal (dSph) galaxies. The gas-deficient dSphs as well as dwarf ellipticals (dEs) are typically found in close proximity to one of the large spirals, whereas most of the gas-rich, star-forming dwarf irregulars (dIrrs) are located at larger distances. For a review of the properties of different types of dwarf galaxies, see Grebel (2001). Evidence for minor merger events, either in the form of ongoing interactions

ludwig@ari.uni-heidelberg.de

or relics in the form of vast tidal streams, is found in and around the MW (e.g., Ibata et al. 1994; Yanny et al. 2003; Duffau et al. 2006; Bell et al. 2008; Williams et al. 2011) and M31 (e.g., Ibata et al. 2001; Zucker et al. 2004; Chapman et al. 2008; McConnachie et al. 2009; Mackey et al. 2010).

Other nearby groups also show structures dominated by two or more moderately massive galaxies with an extended entourage of dwarfs (e.g., Karachentsev et al. 2002a,b, 2003a,b,d; Chiboucas et al. 2009). For galaxy groups beyond 5 Mpc, usually less detailed information is available, with past efforts having focused mainly on global properties (e.g., Trentham et al. 2006; Tully & Trentham 2008; Jacobs et al. 2009; Courtois et al. 2009). Furthermore, prominent tidal streams and morphological perturbations were detected around individual nearby spiral and elliptical galaxies (Schweizer & Seitzer 1988; Malin & Hadley 1999; Martínez-Delgado et al. 2009, 2010; Mouhcine et al. 2010, 2011; Mouhcine & Ibata 2009; Miskolczi et al. 2011) or on larger scales in, e.g., the interacting M81 group (e.g., Yun et al. 1994; Makarova et al. 2002).

The galaxy content at the faint end of the luminosity function and the presence or absence of tidal streams and substructure allow us to visualize different steps of group evolution driven by the environment similar to related studies in galaxy clusters (e.g., Lisker et al. 2006b, 2007; Smith et al. 2009; Paudel et al. 2010). This motivated us to initiate the "Giant GAlaxies, Dwarfs, and Debris Survey" (GGADDS). Our goals are to correlate the observed properties of spiral galaxies and groups to the frequency of tidal interactions, and to characterize the impact of local density on the dwarf galaxy population. GGADDS combines the search for signatures of recent accretion events with the study of dwarf galaxy populations in different types of nearby galaxy groups.

In our current paper, we present the first GGADDS results based on deep imaging of the SAb spiral galaxy NGC 7331 and its surroundings. In Section 2, we introduce the GGADDS project. In Section 3, we describe the observations and data reduction for our first target, NGC 7331. In Section 4, we present our results, followed by a discussion (Section 5) and our conclusions (Section 6).

2. THE GGADDS PROJECT

The GGADDS project concentrates on galaxy groups in the nearby universe within a distance range of ~ 10 to ~ 35 Mpc. The main goal is to detect dwarf galaxy candidates and possible tidal features in order to constrain their properties as a function of environment, and to explore whether links exist between these two aspects of the surroundings of giant galaxies. We currently use deep imaging with small to medium-size optical telescopes (0.9m to 4m-class) to support photometric and structural studies, later to be complemented with spectroscopy. Our selected dominant group galaxies range from $M_B = -19$ to -23 mag and are located in environments with densities varying from 0.08 to 1.6 galaxies Mpc^{-3}.

The distance range of our targets is motivated by our choice of telescopes: at 10 – 35 Mpc, the instrument field of view of commonly used wide-field imagers ($\sim 36' \times 36'$ to $59' \times 59'$) covers an area of typically (175×175) kpc^2 to (611×611) kpc^2, while the instrument sensitivity allows us to reach a limiting surface brightness of 27 mag arcsec^{-2} in the g-band. For comparison, numerical simulations by Johnston et al. (2008) show that tidal streams due to accretion events should be detectable at this surface brightness for minor mergers that occurred in the last Gyr. Minor mergers have baryonic mass ratios $\leq 1:4$ for $M_{satellite}/M_{primary}$ (Lotz et al. 2011).

To test the feasibility of this project we observed NGC 7331, an SAb galaxy at a distance of 14.2 Mpc viewed under an inclination angle $i = 77°$. Its inferred luminosity is $M_B = -20.4$ mag (de Vaucouleurs et al. 1991) and its maximum rotational velocity is (245.5 ± 5.2) km s^{-1} (taken from Hyperleda[1], based on the catalog from Bottinelli et al. 1982). These quantities are similar to the properties of the MW and M31. NGC 7331 contains a large-scale dust ring with a radius of about 6 kpc (Regan et al. 2004) and its observed H I distribution shows a warp in the outskirts of the disk (Bosma 1981). The latter could be a sign of past interactions.

NGC 7331 is located in a sparse group with a density of 0.33 galaxies Mpc^{-3} down to $M_V = -16$ mag (Tully & Fisher 1988). Other luminous group members include the disk galaxies NGC 7217, NGC 7320, NGC 7292, NGC 7457, UGC 12060, UGC 12082, UGC 12212, UGC 12311, and UGC 12404 (see Figure 1). The galaxies of this group are within ± 170 km s^{-1} from NGC 7331, which itself has a radial velocity $v = (816 \pm 1)$ km s^{-1} (Haynes et al. 1998). NGC 7331 is the most luminous galaxy of this group. The other late-type galaxies span the magnitude range $-16 \lesssim M_B \lesssim -20$ mag. In comparison with the Local Group the NGC 7331 group has only one member brighter than $M_B = -20$ mag. The NGC 7331 group is classified as a stable group (Materne & Tammann 1974) and is part of the Pegasus Spur (Tully & Fisher 1988).

Figure 1 gives an overview of the NGC 7331 galaxy group, underlining the loose, extended character of this group, which resembles the nearby Sculptor group (e.g., Karachentsev et al. 2003b). When measuring the projected distances from NGC 7331 to the other members, we get typical distances of 1 Mpc and for the most distant member, UGC 12404, 2.16 Mpc.

3. OBSERVATIONS AND DATA REDUCTION

The observations were performed in 2009 October with the Wisconsin Indiana Yale NOAO (WIYN) 0.9m telescope at Kitt Peak National Observatory in Arizona equipped with the MOSAIC imager. This instrument is a wide-field imager with eight single CCDs, providing a total area of (8192×8192) pixels^2. The total field of view is 1 deg^2 with a pixel scale of $0.43''$ pixel^{-1}.

We imaged NGC 7331 for 3.5 hr (9×1200 s + 2×900 s) in the Sloan Digital Sky Survey (SDSS) g-band and 4.17 hr (11×1200 s + 2×900 s) in the SDSS r-band. The dither pattern was chosen with a step size of $400''$ in right ascension and declination so that the galaxy would lie in each of the central four CCDs.

We reduced the data with IRAF[2] using the MSCRED package, which was specifically developed for the MO-

[1] http://leda.univ-lyon1.fr/

[2] IRAF is distributed by the National Optical Astronomy Ob-

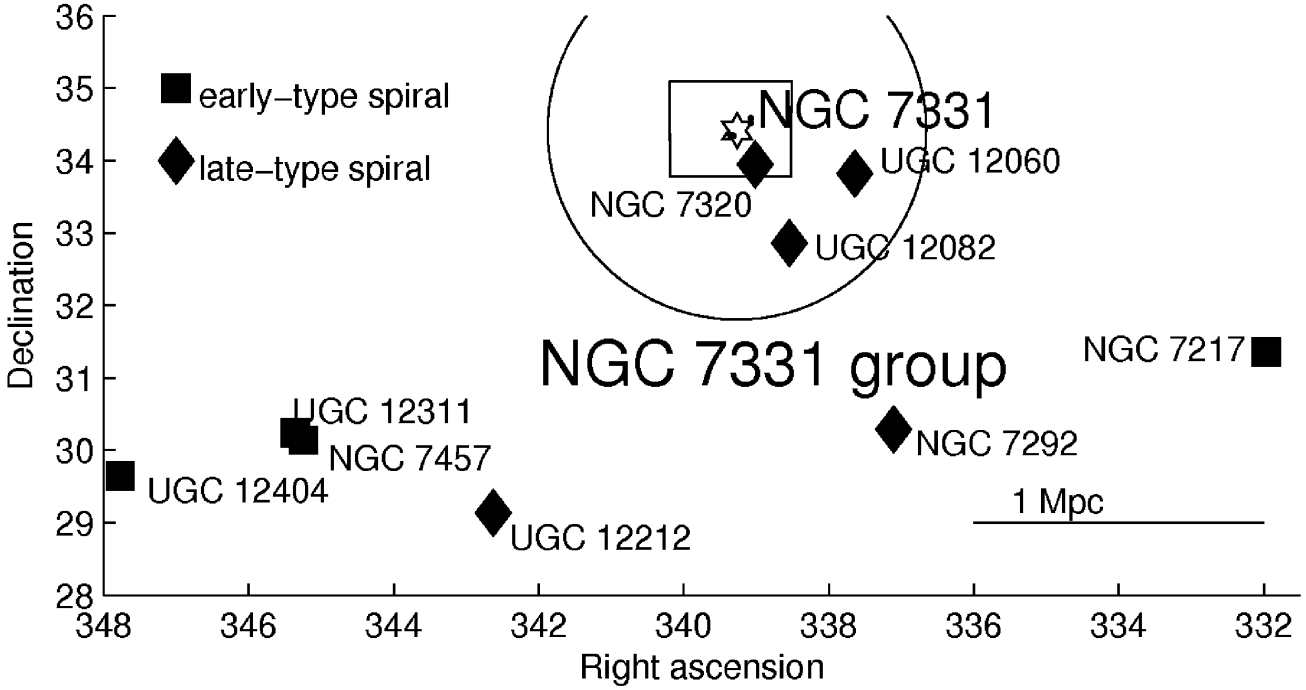

Figure 1. Wider NGC 7331 group environment. The star symbol represents the centroid of NGC 7331. The dots around it are our dwarf galaxy candidates. The open rectangle marks our field of view. Filled squares show other massive, yet less luminous early-type spiral galaxies in the NGC 7331 group and in its immediate surroundings. Filled lozenges show late-type spirals in the group and in its vicinity. The open circle indicates a virial radius of 1.3 Mpc around NGC 7331.

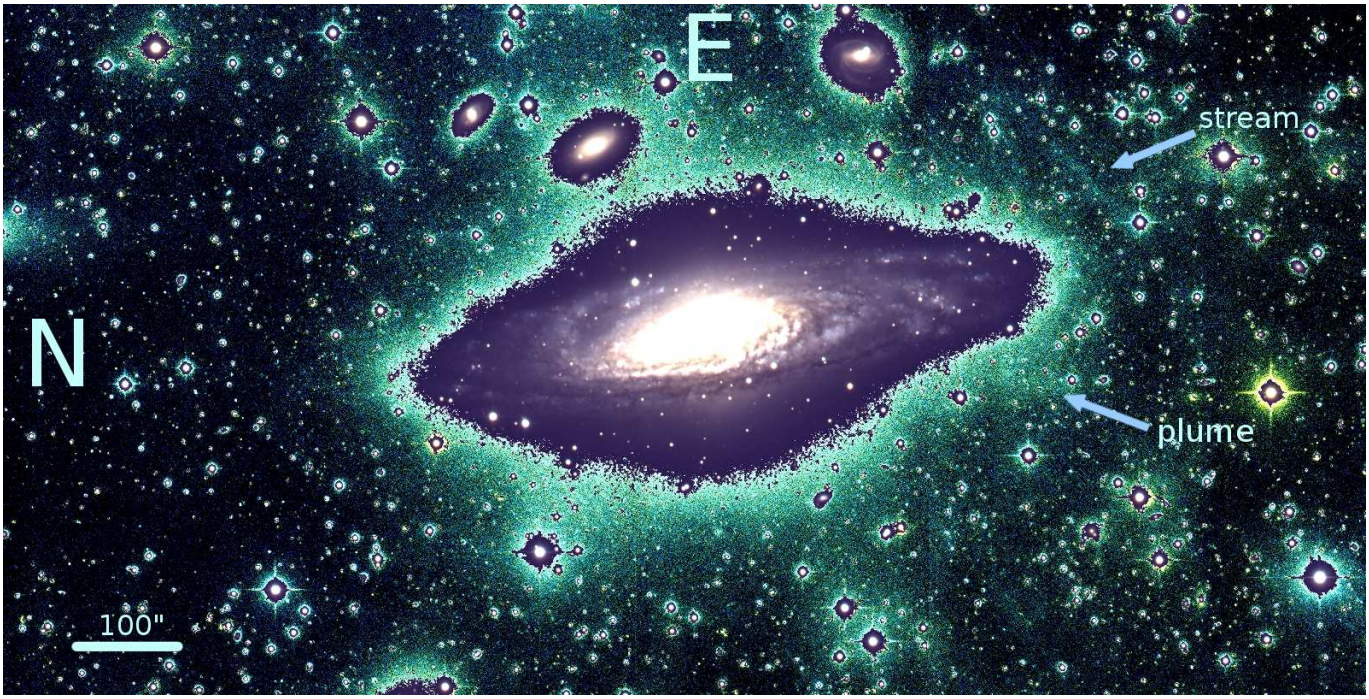

Figure 2. Optical view of the inclined spiral galaxy NGC 7331 (center). The image is composed of deep images in the SDSS g- and r-bands obtained with the 0.9m WIYN telescope and has a total size of $22.5' \times 11.4'$, where $100''$ correspond to 7 kpc. A number of luminous background galaxies and foreground stars are visible as well. The outer, grainy-looking regions are contrast enhanced in order to make faint features visible. In the outskirts, faint tidal debris structure can be seen and is highlighted by the arrows.

SAIC imager. As a first step, the images were corrected for bias and dome flatfields in order to remove the pixel-to-pixel sensitivity variations. We also corrected for the illumination pattern using a "super flat", which was produced by taking the median of the science exposures (making sure to remove the left-over sources), as well as for atmospheric extinction. The images were scaled to the same sky transparency.

We estimated the accuracy of the flat-field correction by comparing the global mode of the background (computed across the overall field of view) with local background modes (calculated in 16 subarrays, each half of the size of a CCD). We measured a typical variation of the background values of about 1.7% in the SDSS r-band and of 2.3% in the g-band.

We used stars from the USNO-B1 catalog (Monet et al. 2003) to derive a world coordinate system (WCS) solution for each CCD in each exposure. The typical accuracy of the transformation from pixel coordinates to equatorial coordinates is $0.2'' - 0.3''$ across the 1 deg^2 field of view. We then ran the IRAF task mscimage to combine all eight CCDs of one exposure into a single mosaic image, reproducing the full field of view of the instrument with a fixed pixel scale of $0.43''$ pixel^{-1}.

Individual mosaic images were subsequently corrected for the airmass with the extinction coefficients provided by the observatory[3] at the central wavelengths of the filters[4].

For each individual image we calculated the mode value of the background across the entire field of view and subtracted it. Furthermore, in order to account for the different transparency of the atmosphere in different nights, we measured the total counts in a non-saturated region centered on NGC 7331. We chose the exposure with the highest counts as reference and scaled the others to this value. We stacked the images by using their WCS solution and normalized the final image by the total exposure map. Due to the dither pattern we obtain a final image size of 11148 pixels × 11756 pixels with a resulting field of view of $1.3^\circ \times 1.4^\circ$, where the edges of the final image have a lower total exposure time (fewer exposures) and a higher noise than the central regions. The area with complete overlap of all stacks is 5440 pixels × 4640 pixels resulting in a field of view of $33' \times 38'$. The final image is characterized by an average point-spread function (PSF) with a full width at half maximum (FWHM) of $1.3''$ in each filter.

For the photometric calibration we used stars in common between our final image and the SDSS Data Release 7 (DR7; Abazajian et al. 2009). We only used stars that are not saturated in our science images but bright enough to have a good signal-to-noise ratio (S/N). In the SDSS g-band we used stars between 16.5 and 18 mag and derived a zero point of (22.24 ± 0.04) mag, while in the SDSS r-band we selected stars between 16 and 17.5 mag and obtained a zero point of (22.19 ± 0.03) mag.

We used the extinction maps of Schlegel et al. (1998) and the extinction law of Cardelli et al. (1989) with $R_V = 3.1$ to calculate the Galactic foreground extinction at the central wavelength of the SDSS g- and r-bands (R_V is the ratio of total to selective extinction in the V-band). All the magnitudes and surface brightnesses derived in the next sections are given already corrected for Galactic foreground extinction.

In deep imaging Galactic cirrus can act as an intervening contaminant. Therefore, the occurrence of cirrus imposes a limit on surface photometry as it is a Galactic foreground that cannot be removed (e.g., Sandage 1976).

In our observed region Galactic cirri are visible. Interestingly cirrus clouds show very red broadband colors (Szomoru & Guhathakurta 1998). Typical $(B-R)$ values range from 1.0 to 1.7 mag (Guhathakurta & Cutri 1994) and translate into $(g-r) = 1.33$ to 2.03 mag when using the color transformation $(B_J - R) = (g-r) + 0.33$ from Fukugita et al. (1995). Therefore, on the basis of their measured colors, faint and blue galaxy features can be distinguished from red Galactic cirrus clouds.

The extinction maps of Schlegel et al. (1998) do not take into account the presence of small scale dust features which can be seen in emission as "cirrus". Therefore our reddening correction does not remove any effect associated with source obscuration by dust associated with cirrus. A careful visual inspection of our images indicates that no cirrus is in close proximity to the objects discussed below, so cirrus reddening is unlikely to be a significant effect.

Observationally, the angular resolution is the most limiting factor for detecting faint, distant dwarf galaxies or streams. Due to the pixel scale of $0.43''$ pixel^{-1} and the need to have several pixels in order to resolve structures we are able to detect objects with a minimum size of 0.3 kpc at the distance of NGC 7331.

4. RESULTS

4.1. *NGC 7331*

A color composite image of NGC 7331 is shown in Figure 2. Two images with different contrast levels are overlaid. The white-blue high-surface-brightness inset shows the brighter regions of NGC 7331, highlighting its overall structure, especially its spiral arms and bulge. The underlying green low S/N image reveals the low-surface-brightness features of the galaxy, including a candidate tidal stream and a plume, which are marked with arrows in Figure 2 and are discussed further below.

4.2. *Identification of Dwarf Galaxy Candidates*

In order to identify possible dwarf galaxy candidates around NGC 7331, a first analysis was done via visual inspection of the science images. We selected dwarf galaxy candidates on the basis of their low apparent surface brightness, diffuse structure, and angular extent of at least $7''$, which is five times the typical PSF. This was necessary in order to be able to distinguish extended objects from point sources. With spectroscopic follow-up studies Chiboucas et al. (2010) confirm that these selection criteria have a good success rate in identifying true dwarf galaxies. Our field of view and sensitivity do in principle permit us to detect all objects within a galactocentric distance of up to 170 kpc around NGC 7331 and down to a surface brightness $\mu_g = 27$ mag arcsec^2.

servatory, which is operated by the Association of Universities for Research in Astronomy, Inc., under cooperative agreement with the National Science Foundation.

[3] The standard extinction values for the Kitt Peak National Observatory can be found in the file kpnoextinct.dat of the task onedstds, which is part of the IRAF package ONEDSPEC

[4] http://www.noao.edu/kpno/mosaic/filters/filters.html

We identified four candidate dwarf galaxies, which we named with capital Latin letters in alphabetical order according to increasing projected distance to NGC 7331. Thus the nearest one is called NGC 7331 A, the second nearest NGC 7331 B, and so forth.

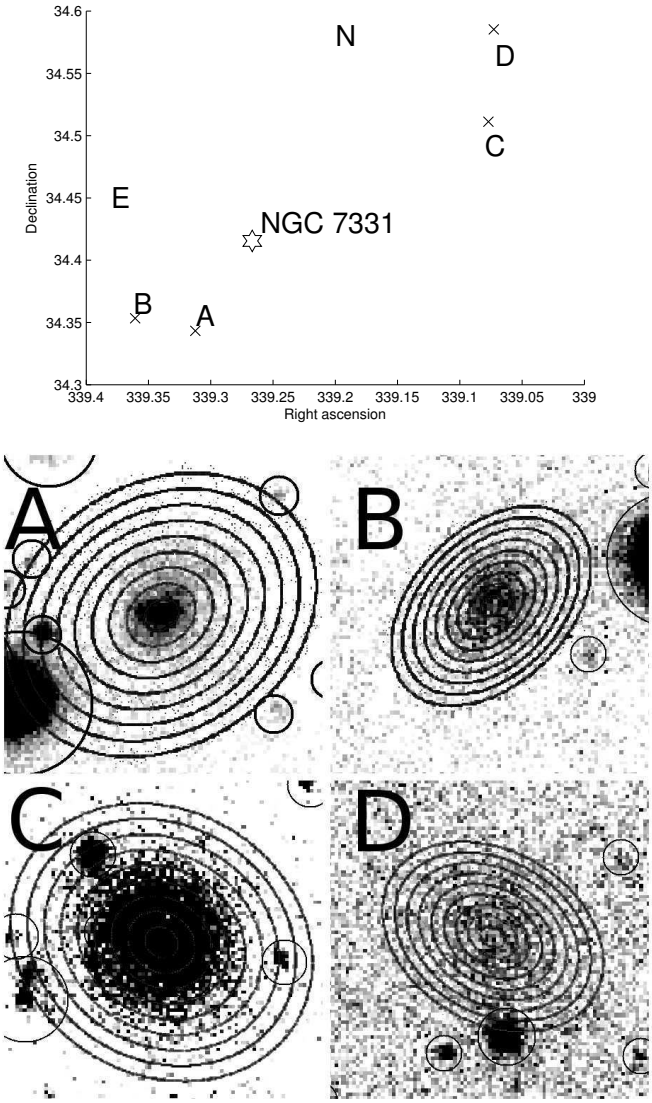

Figure 3. Top: the positions of the dwarf galaxy candidates. Bottom: images of the dwarf galaxy candidates in the SDSS g-band obtained with the WIYN 0.9m telescope. These are cut-outs of the final stacked image of our observations with sizes of 180 pixels × 180 pixels. North is left and east is up. The concentric elliptical annuli centered on each of the dSph candidates indicate a subset of the regions within which the surface brightness was measured. The open circles mark presumed background objects that were masked out.

4.3. *Photometry of the Dwarf Galaxy Candidates*

We ran SExtractor (Bertin & Arnouts 1996) on images with a size of 180 × 180 pixels centered on each candidate in order to measure the integrated g and r magnitudes of the candidates after an accurate estimate of their local background. We configured SExtractor to measure isophotal magnitudes in two different apertures defined by the detection thresholds of 1σ and 3σ above the background. The resulting apparent integrated magnitudes are given in Table 1, together with their errors computed from SExtractor, which also takes into account the uncertainty on the photometric calibration. The absolute magnitudes were calculated assuming the same distance modulus (30.70 ± 0.32 mag) for the dwarf galaxy candidates as for NGC 7331. Their associated errors also include the error in the distance modulus.

We see that these four candidates fall in the magnitude range $-13 \lesssim M_r \lesssim -11$ typical of the classical dSph galaxies in the Local Group (Grebel et al. 2003). We checked the H I data obtained for NGC 7331 by Walter et al. (2008), and found no H I emission at the position of the four candidates, indicating that there may be no gas for future star formation available. This would be consistent with the properties of the majority of known dSphs in the Local Group. Only NGC 7331 A could possibly be classified as a transition object, because its core, being slightly bluer than its outer parts (see Section 4.4), could have recently undergone some star formation.

As the S/N is different for the g- and r-bands, the integrated magnitudes computed by SExtractor sample different areas within each galaxy candidate. In the next section, we will use the IRAF task ellipse to compute the integrated color over the same region for each candidate and filter.

4.4. *Surface Brightness Profiles*

At first we measured the photometric center of our four dwarf candidates with the IRAF tool center in the DIGIPHOT package. The resulting centers are needed to run ellipse, where we kept the ellipticity and position angle parameters fixed at the values measured by eye (see Figure 3).

In order to measure the surface brightness as a function of galactocentric distance along the semi major axis, we set up ellipse to fit a series of concentric isophotes to the stamp images of the four candidates with the length of the semi major axis gradually increasing with a linear step of a factor of 1.1 (see Figure 3).

The surface brightness profiles (SBPs) derived in the r-band are shown in Figure 4 with open circles and the error bars computed by ellipse. The maximum length of their semi major axis is defined by the corresponding surface brightness being just 1σ above the background. To characterize the structural parameters of the four candidates, we fitted their SBPs with the Sérsic profile (Sersic 1968):

$$\mu(r) = \mu_0 + 1.086 * (r/h)^{1/n} \quad (1)$$

(Cellone 1999) where μ is the surface brightness, μ_0 is the central surface brightness, r is the distance from the galaxy center along the semi major axis, h is the scale length and n is the Sérsic index. We cut each SBP at the semi major axis whose corresponding surface brightness is just 3σ (1σ for NGC 7331 D because of its low surface brightness) above the background in order to minimize the uncertainty on the best fitting Sérsic profile. We used a non linear least-squares fit with the Levenberg-Marquardt algorithm. The best fitting Sérsic profiles are plotted in Figure 4 with a solid line, and their parameters

Table 1
Observational Properties of the Dwarf Galaxy Candidates

Property	NGC 7331 A	NGC 7331 B	NGC 7331 C	NGC 7331 D
R.A. [J2000] [h m s] (1)	22:37:14.98	22:37:26.56	22:36:18.49	22:36:17.46
Decl. [J2000] [° m s] (2)	34:20:35.86	34:21:12.23	34:30:40.37	34:35:07.20
g_0 (1σ) (mag) (3)	18.48 ± 0.04	20.01 ± 0.05	18.30 ± 0.04	20.65 ± 0.05
g_0 (3σ) (mag) (4)	19.91 ± 0.04	20.82 ± 0.20	18.53 ± 0.04	—
r_0 (1σ) (mag) (5)	17.80 ± 0.03	18.75 ± 0.03	17.58 ± 0.03	20.21 ± 0.04
r_0 (3σ) (mag) (6)	19.14 ± 0.03	19.75 ± 0.03	17.90 ± 0.03	—
A_g (mag) (7)	0.34	0.32	0.33	0.33
A_r (mag) (8)	0.25	0.23	0.24	0.24
$(g-r)_0$ (1σ) (mag) (9)	0.57 ± 0.05	0.63 ± 0.06	0.55 ± 0.05	0.75 ± 0.06
$(g-r)_0$ (3σ) (mag) (9)	0.39 ± 0.05	0.62 ± 0.20	0.54 ± 0.05	—
$\mu_0(r)$ (mag arcsec^{-2}) (10)	23.33 ± 0.10	24.10 ± 0.06	23.76 ± 0.03	25.20 ± 0.08
h_r (pc) (11)	325 ± 33	456 ± 15	592 ± 16	516 ± 27
n (12)	1.28 ± 0.11	0.62 ± 0.07	0.71 ± 0.03	0.52 ± 0.07
M_r (1σ) (mag) (13)	-12.90 ± 0.32	-11.95 ± 0.32	-13.12 ± 0.32	-10.48 ± 0.32
R(NGC 7331)$_{\rm projected}$ (kpc) (14)	20 ± 2	25 ± 3	45 ± 5	58 ± 7

Rows (1) and (2) are the coordinates (J2000 right ascension and declination) where we give hours, minutes, and seconds in row (1) and degrees, minutes, and seconds in row (2). Rows (3) – (6) are the apparent magnitudes in the SDSS g- and r-band with 1σ and 3σ thresholds above the background detections. In rows (7) and (8), A_g and A_r are the extinction values for the SDSS g- and r-band. Row (9) contains the extinction-corrected color in the SDSS g- and r-bands. Row (10) shows the central surface brightness in the r-band, $\mu_0(r)$. Row (11) lists the exponential scale length, h_r. Row (12) provides the Sérsic index; n, row (13) the absolute magnitude in the r-band, M_r, when assuming a distance modulus of 30.70± 0.32; and row (14) the projected distance to NGC 7331, R.

(n, μ_0, h_r) are shown in Table 1.

The Sérsic indices n obtained for the four candidates range from 0.5 to 1.3, and are in good agreement with those measured by Chiboucas et al. (2009) for the dSphs and dIrrs in the M81 group ($0.21 \lesssim n \lesssim 1.0$). The estimated μ_0 of the four candidates varies between 23 and 25 mag arcsec^{-2} and is consistent with the central surface brightness of the dwarfs in the M81 group as derived by Chiboucas et al. (2009).

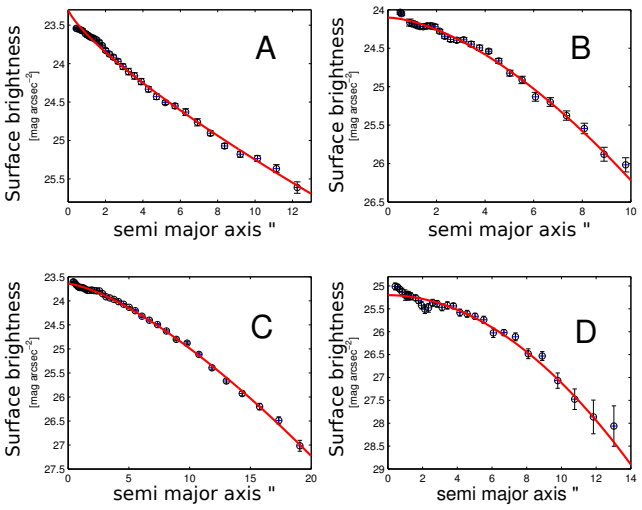

Figure 4. Surface brightness profile fits to the dwarf galaxy candidates of NGC 7331 in the SDSS r-band.

We used the SBPs to determine the semi major axes $r_{1\sigma}$ and $r_{3\sigma}$ at which μ is just 1σ and 3σ, respectively, above the background. For our data, $r_{1\sigma}$ and $r_{3\sigma}$ are smaller in the g-band, therefore we used their values in the g-band ($5.5'' < r_{1\sigma} < 11.0''$ and $2.5'' < r_{3\sigma} < 9.0$) to compute the integrated $(g-r)_0$ colors of each candidate. These colors are reported in Table 1.

For each candidate except NGC 7331 A, the colors derived for the 1σ and 3σ thresholds are very similar; in the case of NGC 7331 A the color for the 3σ threshold is bluer than that for 1σ. This indicates that this galaxy is bluer in its center, perhaps akin to what is observed in some of the more massive "blue-core dwarf ellipticals" (dE(bc) as classified by Lisker et al. 2006a) in the Virgo cluster. For these dE(bc) galaxies, Lisker et al. (2006a) were able to show spectroscopically that they did experience star formation in their centers less than a Gyr ago. Similar examples – again among the more luminous dEs – are also known from the Local Group, where the close M31 dE companions NGC 185 (e.g., Hodge 1963; Butler & Martínez-Delgado 2005) and NGC 205 (e.g., Cappellari et al. 1999; Monaco et al. 2009) show recent star formation in their centers. NGC 7331 A may be a lower-luminosity nucleated dSph counterpart of these systems. Note that some Galactic dSph galaxies, in particular Fornax, also show relatively recent star formation that occurred just a few 100 Myr ago, though at the current time they are no longer active (Grebel & Stetson 1999; Saviane et al. 2000).

The $(g-r)_0$ colors of the four dSph candidates around NGC 7331 range from 0.55 to 0.75 mag. In order to compare them with the dwarfs in the Local Group, we used the color transformation equations from Jordi et al. (2006) for Population II stars to translate the $(g-r)_0$ colors of the four candidates into $(B-V)$ colors, i.e., we apply the transformation relation $(B-V) = 0.918 \cdot (g-r) + 0.224$. The resulting $(B-V)$ values vary between 0.7 and 0.9 mag and are consistent with the $(B-V)$ colors measured for LGS 3, And I and Leo I in the Local Group (Mateo 1998).

4.5. *Dwarf Galaxy Candidates in the SDSS*

We checked that the four dwarf galaxy candidates found in our WIYN data are also visible in the SDSS images available for NGC 7331. We were able to recover them, although they have a much lower S/N in the SDSS data than in our own data. With a detection limit of $\mu_0(g) \approx 27.0$ mag arcsec^{-2} the WIYN data are slightly deeper than the SDSS in the individual filters.

According to the NASA Extragalactic Database (NED[5]), NGC 7331 has the same morphological type as M31, yet is more than 1 mag brighter in the optical (V-band) and in the near-infrared (H-band). It may thus be more massive than M31 (see also Section 5.1). We then might expect it to be surrounded by a number of close dE companions similar to those found near M31. Interestingly we did not detect any bright dE across of the field of view of our WIYN data. We then decided to search for dE candidates in the SDSS images covering the surroundings of NGC 7331 out to a distance of 1 Mpc. The depth of the SDSS imaging data in the g-band reaches surface brightnesses as faint as $\mu_0(g) \approx 26.0$ mag arcsec^{-2} – 26.5 mag arcsec^{-2} (Kniazev et al. 2004). Therefore dEs, which have a typical μ_r between 21 and 24 mag arcsec^{-2} and a $(g-r)$ color between 0.2 and 0.8 mag (Lisker et al. 2007, 2008), should be easily detectable in the SDSS images.

We retrieved from the SDSS DR7 photometric catalog (Abazajian et al. 2009) all objects with a Petrosian radius larger than 10″, $0 \lesssim (g-r) \lesssim 1.5$ mag, and 21 mag arcsec^{-2} $\lesssim \mu_g \lesssim$ 26 mag arcsec^{-2}, in order to sample the parameter space of dEs and dSphs. The limits in color and surface brightness were chosen from the properties of dEs in the Virgo Cluster (Lisker et al. 2007, 2008). Smaller Petrosian radii do not allow one to carry out a proper analysis of the object's morphology. A visual inspection of the selected objects revealed no dE or bright dSph candidates.

4.6. *Analysis of the Stellar Stream*

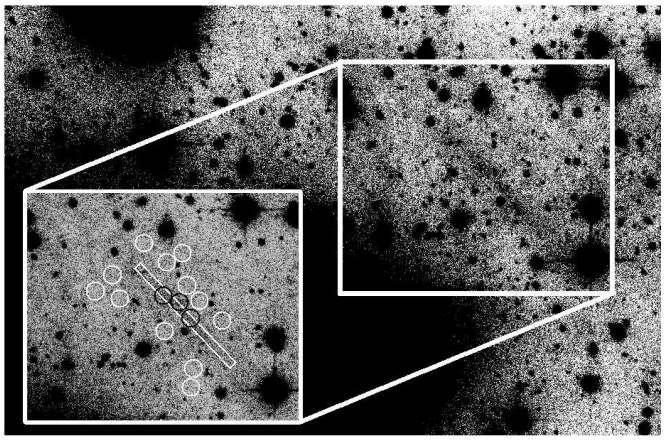

Figure 5. Faint stellar stream near NGC 7331. The inset shows the analyzed region. The black circles mark the brightest regions of the stream where we measured the magnitudes and white circles represent the areas of the local background estimation. The white rectangle indicates the region where the color profile was measured.

In the south eastern outer regions of NGC 7331, we find hints of a very low surface brightness structure in our WIYN images that we interpret as a stellar stream (Figure 5). We measured the length of the stream with the SAOImage DS9 tool 'projection' by placing a rectangular aperture, 29″× 85″, along the stream in a combined g-and r-band image. This gives the mean counts along the stream. This produced an average brightness profile of the stream, and its length was estimated as the distance between the two edges of the stream where the brightness is less than 1σ above the background.

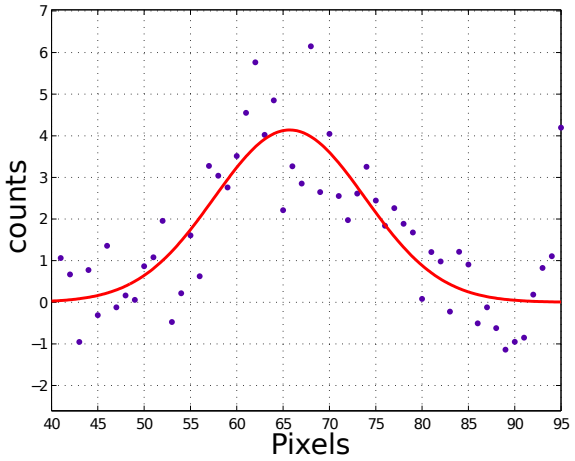

Figure 6. Gaussian fit to the width of stream. For the fit, we used the stacked g- and r-band images.

Similarly, we determined the width of the stream with a box of 29″× 65″ placed across the stream in a region free of bright stars. The resulting brightness profile was fitted with a Gaussian function (see Figure 6). Its FWHM was used to define the width of the stream. In this manner we obtained a length of 5 kpc and a width of 802 pc for the stream (assuming the same distance modulus as for NGC 7331).

We defined a set of twelve circular apertures, 10″ in diameter, to estimate an average background in the surroundings of the stream, and three apertures of the same size centered on the brightest regions of the stream to derive its surface brightness. After correcting for the local background, we obtained $\mu_{g,0} = (26.88 \pm 0.11)$ mag arcsec^{-2}, $\mu_{r,0} = (26.63 \pm 0.10)$ mag arcsec^{-2}, and $(g-r)_0 = (0.16 \pm 0.16)$ mag, at an S/N of about 7. We discuss the possible origin of the stellar stream in Section 5.

Since many dwarf galaxies in groups and clusters show color gradients (e.g., Kormendy & Djorgovski 1989; Chaboyer 1994; Harbeck et al. 2001), it is interesting to check whether the stream also shows such a color variation. In order to do so we used pvector on an area of 354 kpc ×5 kpc aligned with the stream and extracted the average surface brightness of the stream in each filter (see Figure 5). The resulting color profile is plotted in the top panel of Figure 7, where the solid line represents the mean color obtained after a 1 σ clipping of the data. We also binned the color profile with a bin size of 13 pixels in order to improve the S/N; the result is shown in the bottom panel in Figure 7, where the solid line traces again the average color across the stream (0.15 ± 0.06 mag). This is in good agreement with the color previously obtained with aperture photometry. Integrating the SBP of the stream we derived $g_0 = (20.03 \pm 0.46)$ mag and $r_0 = (19.87 \pm 0.69)$ mag corresponding to $M_r = (-10.83 \pm 0.76)$ mag at the distance of NGC 7331.

We also checked the SDSS images in the g- ,r-, and i-

[5] URL: http://ned.ipac.caltech.edu

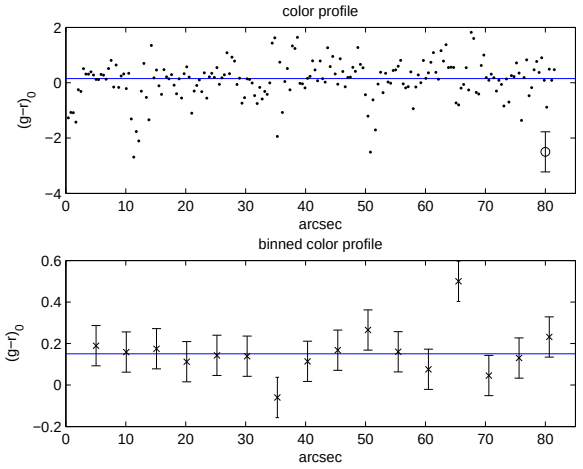

Figure 7. Color profile of the stream. The upper plot shows the individual color estimates per pixel. The bottom plot is binned with a bin size of 13 pixels. In both panels, the line represents the calculated mean. Within the 1σ errors no color gradient can be detected.

bands, but we were not able to clearly detect the stream. Also the stacked *gri*-band image does not show a recognizable stream, indicating that the SDSS data are not deep enough and do not provide a high enough S/N to study the stream.

In addition to the stream, another faint feature – a plume – can be detected in the southwest outer regions of NGC 7331 (see Figure 2). We performed aperture photometry (three apertures with $r = 5''$) of the plume and derived average surface brightnesses of these apertures of $\mu_{g_0} = (26.29 \pm 0.46)$ mag and $\mu_{r_0} = (25.79 \pm 0.30)$ mag with a resulting color of $(g-r)_0 = 0.50 \pm 0.17$. The errors correspond to the fluctuations of the calculated magnitudes in the different apertures. In its surface brightness this feature is similar to the northern spur that can be seen around M31 (Ferguson et al. 2002). This feature could be the result of another accretion event. Given their relatively blue colors, the stream and the plume cannot be mistaken for Galactic cirrus clouds, because, as discussed in Section 3, the latter have a typical $g - r$ color between 1.3 and 2 mag.

5. DISCUSSION

Hierarchical models of galaxy evolution (e.g., White & Frenk 1991) suggest that the halos of giant galaxies contain large numbers of low-mass dark matter halos. If populated by baryonic matter as well, these halos may be observable as dwarf galaxies. It is well established, however, that even in the case of the MW the number of known dwarf companions is less than the predicted number of satellite halos (e.g., Moore et al. 1999; Kravtsov 2010). While observations of the Local Group and other nearby groups (e.g., Karachentsev 2005) show a high number of dwarf galaxy companions and some tidal interactions (e.g., Miskolczi et al. 2011), the numbers are consistently lower than the model predictions. This missing satellite problem indicates that on the mass scale of galaxies, observations do not reveal luminous versions of the expected substructures.

The possibility therefore exists that only a minority of low-mass satellite dark matter halos contain stars (e.g., Madau et al. 2008). An interesting question is how common such observable luminous structures are, and whether they follow well-defined patterns associated with either host galaxy or galaxy group properties in the nearby universe. Thus we selected nearby galaxy groups for study in GGADDS as these provide the most common environments within which sub-halos should exist in the present-day universe.

5.1. *The NGC 7331 Galaxy Group*

NGC 7331 is a member of a filamentary group of galaxies (see Figure 1). It contains two giant spirals, NGC 7217 and NGC 7331, as well as the luminous S0 galaxy NGC 7457. If we consider the virial radii of typical galaxy groups to be $R_{vir} \leq 1.3$ Mpc (Karachentsev 2005), then the NGC 7331 group appears to consist of three subgroups: (1) the relatively empty zone surrounding the SAb galaxy NGC 7217; (2) a subsystem containing the late-type galaxies NGC 7320, UGC 12060, and UGC 12082 associated with NGC 7331; and (3) a third grouping around the S0 galaxy NGC 7457, which is accompanied by a dwarf S0/dE. The NGC 7457 subgroup is noteworthy in containing early-type disk galaxies, suggesting that it is dynamically more evolved. In contrast to that the NGC 7331 subgroup is dominated by gas-rich late-type galaxies, indicating that it is likely to be in an earlier dynamical evolutionary phase (see Figure 8).

Overall, the NGC 7331 subgroup therefore resembles the loose groupings of late-type giant galaxies found in the Sculptor group or the Canes Venatici cloud (Jerjen et al. 1998; Karachentsev et al. 2003b,c; Karachentsev 2005). Karachentsev (2005) finds that the M94 group and the Sculptor group are not in a state of dynamical equilibrium, a situation that likely applies to the overall NGC 7331 group. In comparison the Local Group, with its two giant spirals separated by ~ 0.8 Mpc, is a denser and likely more massive galaxy group than the NGC 7331 subgroup. Such a more massive and richer galaxy group should have a shorter crossing time, and offer more opportunities for internal interactions within the typical group radius of approximately 1 Mpc.

5.2. *The NGC 7331 Dwarf Sample Compared to M31 and Other Nearby Galaxies*

Our study of the region surrounding NGC 7331 reveals four candidate dwarf companions. Three of them have $M_r \leq -13$ mag and are located within a projected radius of 160 kpc from NGC 7331. As this corresponds to the same region covered by the main Pan-Andromeda Archaeological Survey (Richardson et al. 2011), it is interesting to compare results. With our sensitivity we would detect the compact elliptical satellite M32 and all three bright dEs around M31 (i.e., NGC 147, NGC 185, and NGC 205). Obviously any counterparts of such galaxies are missing from our survey zone surrounding NGC 7331. We would also detect at least two of the brighter M31 dSph companions, And I and And II; thus our data are suggestive of roughly comparable luminous dSph populations in the two systems. This result is re-enforced by our finding that the NGC 7331 dwarf galaxy candidates have colors and structures of typical dSph galaxies.

As the absolute H-band magnitude for NGC 7331 (Aaronson 1977) is ≈ 1 mag brighter than that for M31, it is likely that M31 has less stellar mass than

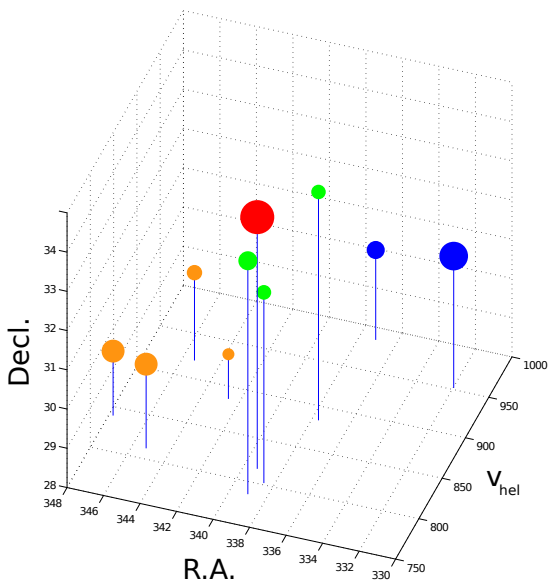

Figure 8. Overview of the NGC 7331 group. The red dot stands for NGC 7331. The blue dots mark the subgroup around NGC 7217, the green ones show other spiral and irregular galaxies belonging to the NGC 7331 subgroup, and the yellow dots indicate the NGC 7457 subgroup (the dot size represents the luminosity of each galaxy). The right ascension (R.A.) and the declination (Decl.) are given in degrees. The heliocentric velocity, v_{hel} is given in km s^{-1}.

NGC 7331. In addition the bulge-to-disk luminosity ratio for NGC 7331 is B/D ≈1 (Bottema 1999) versus B/D ≈ 0.5 for M31 (Geehan et al. 2006). Thus if the dSph population were tied to bulge luminosity, we might expect richer dwarf populations in NGC 7331 as compared to M31. Yet apparently this is not the case, at least within our magnitude limit and with $R \leq 160$ kpc. The deficiency of early-type dwarf satellites associated with NGC 7331, however, is more pronounced if we consider the lack of equivalents to the three classical, luminous dE M31 companions. If we compare the stellar masses of more luminous early-type dwarf companions, excluding the anomalous M32 system, then the detected stellar mass in the form of candidate satellite galaxies around NGC 7331 is about 2% of that found in the same radius and absolute magnitude limit around M31. It thus seems possible that the presence of dE-type satellites could be linked to some parameter other than the (stellar) mass of the host galaxy, such as group density, as suggested by earlier studies (e.g., Ferguson & Sandage 1991).

We conclude that unless dE companions to NGC 7331 have been missed at larger radii, where they should have been detected as candidate dwarfs in the SDSS images, NGC 7331 has substantially less stellar material in the form of satellites than the less massive M31 system. Moreover, NGC 7331 lacks luminous nearby companions like the Magellanic Clouds around the MW. Such irregular companions, however, are generally found to be rare (e.g., Guo et al. 2011).

The statistics for dSphs with $M_r \leq -14$ are not well constrained. Our few detections only sample the counterparts of the most luminous counterparts of the "classical" dSphs in the Local Group. When comparing NGC 7331 and M31 in this respect, it seems possible that similarly numerous populations of such dSph satellites may exist around both spiral galaxies. The differences and similarities between the populations of inner satellite galaxies around NGC 7331 as well as in the Sculptor group and in the Local Group are further illustrated in Figure 9.

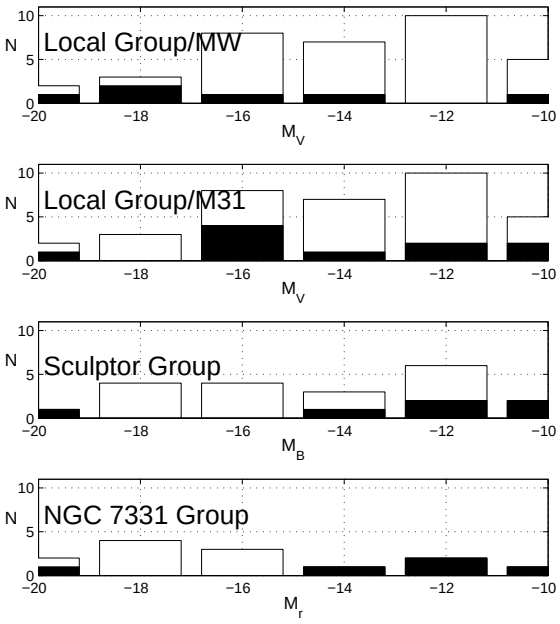

Figure 9. Luminosity function of the NGC 7331 subgroup (bottom panel) compared to the Milky Way and M31 subgroups in the Local Group (upper two panels) and the NGC 253 subgroup in the Sculptor group (third panel). The white (unfilled) histogram bars show the total number of detected member galaxies in a given group. The black (filled) histogram bars in the panels indicate what we would measure if we take into account only the likely dwarf satellites of one massive disk galaxy (the Milky Way and M31 for the Local Group and NGC 253 for Sculptor) to permit a direct comparison with NGC 7331.

5.3. *The Stellar Stream*

Stellar streams extending out of the planes of disk galaxies are well established as indicators of past interactions. Given the low density of the NGC 7331 galaxy group, the presence of stellar streams in NGC 7331 then is somewhat surprising. We focus our discussion on the western stream, but note that additional features are seen to the southwest of the galaxy. As the streams appear to be discontinuous and given that the estimated color of the southwestern feature is different from that of the western stream, we cannot tell whether these are two parts of one single stream or constitute two separate structures.

If the western stellar stream is tidal debris, then the galaxy producing it might be detectable. A system with the luminosity of $M_r = -10.8$ mag that we measured in the western stream segment located away from the obscuring main body of NGC 7331 would be included in our sample, but obviously was not found. The blue color

of this stream segment, $(g-r)_0 = 0.15$ mag, suggests that it might have been produced by a star-forming galaxy (possibly a dIrr or a dIrr/dSph transition-type galaxy), even though no H I is seen today to be associated with the stream. The narrow projected width of the NGC 7331 stream indicates that such a progenitor would have had a low internal stellar velocity dispersion (Johnston et al. 2008). We thus speculate that the accreted galaxy could have been a low-mass dIrr or dIrr/dSph transition-type galaxy, consistent with the modest luminosity and low surface brightness ($\mu_{r,0} = 26.6 \pm 0.1$ mag arcsec^{-2}) of the western stream segment.

According to the color transformations of Fukugita et al. (1995) [$(B - V) = (g - r) + 0.07$, computed for irregular galaxies], the $(g - r)$ color of the stream translates into $(B - V) = 0.23$ mag, comparable with the colors of the bluest dIrrs in the Local Group (e.g., DDO210, Leo A, Sex A, SagDIG from Mateo 1998). The observed blue color could alternatively be produced by old, extremely metal-poor stellar populations, which in addition may possess very blue horizontal branches. However, a comparison with the integrated $B - V$ colors of Galactic globular clusters from Harris (1996, 2010 edition) does not reveal any comparable objects even at low metallicities. The ultra-compact dSph galaxies detected around the MW in recent years (e.g., Zucker et al. 2006; Belokurov et al. 2006) tend to be even more metal-poor than globular clusters, but contain so few stars that they would not leave a recognizable stellar stream with the surface brightness of our stream candidate. The blue color of the stream could also indicate tidally triggered star formation caused by the disruption event if indeed the progenitor was a gas-rich dIrr galaxy. Such young stellar debris was found, for instance, in the halo of the peculiar elliptical galaxy NGC 5128 (Centaurus A), and its A-star colors resemble those of our candidate (Peng et al. 2002).

The timescale since formation of the stream is uncertain. If the NGC 7331 stream is the result of an interaction with a gas-rich dwarf contributing either young blue stars or undergoing tidally triggered star formation, which might suggest a fairly recent interaction a few Myr ago (see Peng et al. 2002). In the Local Group, stars with ages possibly as young as 800 Myr have been detected in the central regions of the Sgr dSph galaxy (Siegel et al. 2007), which is merging with the MW. These stars formed long *after* Sgr began disrupting, but represent only a tiny fraction of the overall stellar populations of Sgr. In any case, interactions involving or leading to recent star formation may not be unusual. Alternatively, such a blue feature might, in principle, form from gas accreted from an intra-group medium. But the observed narrowness of the stream makes this scenario questionable. While star formation has been observed in tidal debris (Makarova et al. 2002; de Mello et al. 2008; Werk et al. 2008), to our knowledge it is not seen in the cases where *diffuse* H I is thought to be accreted onto galaxies (e.g., Sancisi et al. 2008), and therefore is a less likely possibility.

6. CONCLUSIONS

We present the first results from GGADDS in the form of a survey for candidate tidal features and dwarf galaxies in a 160 kpc radius region surrounding the giant SAb spiral NGC 7331, located at an approximate distance of 14.2 Mpc. NGC 7331 is the primary member of a subgroup within a larger filamentary and relatively diffuse galaxy group of the same name. Our deep g- and r-band images reveal four dwarf galaxy candidates that have colors and structures consistent with dSph satellites close to NGC 7331. No examples of more luminous dE-like companions are found. Moreover, a faint western stellar stream is detected, which has a blue color and low surface brightness, possibly indicative of having had a star-forming, low-mass dIrr/dSph transition-type galaxy or a gas-rich dIrr undergoing tidally triggered star formation as its progenitor. There is also a more diffuse and less well-defined feature to the southwest, but it is unclear whether it is connected with the western stream.

Even though NGC 7331 is a giant spiral with higher total and bulge luminosities than M31, it apparently lacks M31's retinue of comparatively luminous dE satellites, as well as something like its compact elliptical companion M32. The absence of such luminous, massive dE companions means that the stellar mass in the form of inner satellites is 2% or less of that around M31.

On the other hand, our few candidate dSph detections are consistent with NGC 7331 and M31 having comparable populations of (classical) dSph companions. The results of our study therefore agree with surveys showing highly variable numbers of moderate-luminosity satellites of giant galaxies, while suggesting that dSph satellites may be more closely tied to the properties of the main galaxy. The source of the large variance in spheroidal satellite stellar masses in galaxy groups remains an interesting question and a potential clue to the origin of these galaxies.

Given the paucity of neighboring galaxies, the detection of what appears to be a bluish stellar tidal debris stream is unexpected. The most straightforward explanation is that NGC 7331 interacted with and at least partially disrupted a star-forming low-mass transition-type dwarf, or that the accretion of a gas-rich dIrr triggered star formation. One of the four dSph candidates discovered in our study shows a blue core similar to more massive, nucleated dEs with recent central star formation found in the Virgo cluster, or similar to transition-type dwarfs with residual centralized star formation activity as observed in the Local Group. Deeper optical and H I observations would be useful in order to obtain a better understanding of the dwarfs and stream(s) around NGC 7331. In low-density groups like the diffuse, extended NGC 7331 group with its many late-type galaxies, interactions with gas-rich dwarfs may be more common than in higher-density environments.

ACKNOWLEDGEMENTS

We thank the anonymous referee for useful comments, which helped to improve this paper. We acknowledge the WIYN Consortium for providing telescope time for this project and for maintaining the WIYN 0.9-m Observatory, along with Hillary Mathis for her support of the Observatory. We are also grateful to the Heidelberg Graduate School of Fundamental Physics (DFG grant No. GSC 129/1), which provided funding for a research visit to Madison, and to the University of Wisconsin-Madison Graduate School for partial support of this research. This research made use of the HYPERLEDA

database (Paturel et al. 2003) and the NASA/IPAC Extragalactic Database (NED) which is operated by the Jet Propulsion Laboratory, California Institute of Technology, under contract with the National Aeronautics and Space Administration.

REFERENCES

Aaronson, M. 1977, PhD thesis, Harvard University, Cambridge, MA.
Abazajian, K. N., et al. 2009, ApJS, 182, 543
Bell, E. F., et al. 2008, ApJ, 680, 295
Belokurov, V., et al. 2006, ApJ, 647, L111
—. 2007, ApJ, 654, 897
Bertin, E., & Arnouts, S. 1996, A&AS, 117, 393
Bosma, A. 1981, AJ, 86, 1791
Bottema, R. 1999, A&A, 348, 77
Bottinelli, L., Gouguenheim, L., & Paturel, G. 1982, A&AS, 47, 171
Butler, D. J., & Martínez-Delgado, D. 2005, AJ, 129, 2217
Cappellari, M., Bertola, F., Burstein, D., Buson, L. M., Greggio, L., & Renzini, A. 1999, ApJ, 515, L17
Cardelli, J. A., Clayton, G. C., & Mathis, J. S. 1989, ApJ, 345, 245
Cellone, S. A. 1999, A&A, 345, 403
Chaboyer, B. 1994, in European Southern Observatory Conference and Workshop Proceedings 49, Vol. 49, Dwarf galaxies, ed. G. Meylan & P. Prugniel, 485
Chapman, S. C., et al. 2008, MNRAS, 390, 1437
Chiboucas, K., Karachentsev, I. D., & Tully, R. B. 2009, AJ, 137, 3009
Chiboucas, K., Tully, R. B., Marzke, R. O., Trentham, N., Ferguson, H. C., Hammer, D., Carter, D., & Khosroshahi, H. 2010, ApJ, 723, 251
Courtois, H. M., Tully, R. B., Fisher, J. R., Bonhomme, N., Zavodny, M., & Barnes, A. 2009, AJ, 138, 1938
de Mello, D. F., Smith, L. J., Sabbi, E., Gallagher, J. S., Mountain, M., & Harbeck, D. R. 2008, AJ, 135, 548
de Vaucouleurs, G., de Vaucouleurs, A., Corwin, Jr., H. G., Buta, R. J., Paturel, G., & Fouque, P. 1991, Third Reference Catalogue of Bright Galaxies (New York: Springer)
D'Onghia, E., Sommer-Larsen, J., Romeo, A. D., Burkert, A., Pedersen, K., Portinari, L., & Rasmussen, J. 2005, ApJ, 630, L109
Dressler, A. 1980, ApJ, 236, 351
Duffau, S., Zinn, R., Vivas, A. K., Carraro, G., Méndez, R. A., Winnick, R., & Gallart, C. 2006, ApJ, 636, L97
Einasto, J., Saar, E., Kaasik, A., & Chernin, A. D. 1974, Nature, 252, 111
Eke, V. R., Baugh, C. M., Cole, S., Frenk, C. S., King, H. M., & Peacock, J. A. 2005, MNRAS, 362, 1233
Ferguson, A. M. N., Irwin, M. J., Ibata, R. A., Lewis, G. F., & Tanvir, N. R. 2002, AJ, 124, 1452
Ferguson, H. C., & Sandage, A. 1991, AJ, 101, 765
Fukugita, M., Shimasaku, K., & Ichikawa, T. 1995, PASP, 107, 945
Geehan, J. J., Fardal, M. A., Babul, A., & Guhathakurta, P. 2006, MNRAS, 366, 996
Girardi, M., Rigoni, E., Mardirossian, F., & Mezzetti, M. 2003, A&A, 406, 403
Grebel, E. K. 1997, in Reviews in Modern Astronomy, 10, ed. R. E. Schielicke, 29–60
Grebel, E. K. 2001, Astrophysics and Space Science Supplement, 277, 231
Grebel, E. K. 2007, in ESO astrophysics symposia, Groups of Galaxies in the Nearby Universe, ed. I. Saviane, V. D. Ivanov, & J. Borissova (Berlin: Springer Verlag), 3
Grebel, E. K., Gallagher, III, J. S., & Harbeck, D. 2003, AJ, 125, 1926
Grebel, E. K., & Stetson, P. B. 1999, in The Stellar Content of Local Group Galaxies, ed. P. Whitelock & R. Cannon, IAU Symposium, 192, 165
Guhathakurta, P., & Cutri, R. M. 1994, in The First Symposium on the Infrared Cirrus and Diffuse Interstellar Clouds, ed. R. M. Cutri & W. B. Latter, ASP Conf. Ser., 58 (San Francisco, CA: ASP), 34
Guo, Q., Cole, S., Eke, V., & Frenk, C. 2011, MNRAS, 417, 370
Harbeck, D., et al. 2001, AJ, 122, 3092
Harris, W. E. 1996, AJ, 112, 1487
Haynes, M. P., van Zee, L., Hogg, D. E., Roberts, M. S., & Maddalena, R. J. 1998, AJ, 115, 62
Hodge, P. W. 1963, AJ, 68, 691
Ibata, R., Irwin, M., Lewis, G., Ferguson, A. M. N., & Tanvir, N. 2001, Nature, 412, 49
Ibata, R. A., Gilmore, G., & Irwin, M. J. 1994, Nature, 370, 194
Jacobs, B. A., Rizzi, L., Tully, R. B., Shaya, E. J., Makarov, D. I., & Makarova, L. 2009, AJ, 138, 332
Jerjen, H., Freeman, K. C., & Binggeli, B. 1998, AJ, 116, 2873
Johnston, K. V., Bullock, J. S., Sharma, S., Font, A., Robertson, B. E., & Leitner, S. N. 2008, ApJ, 689, 936
Jones, L. R., Ponman, T. J., Horton, A., Babul, A., Ebeling, H., & Burke, D. J. 2003, MNRAS, 343, 627
Jordi, K., Grebel, E. K., & Ammon, K. 2006, A&A, 460, 339
Karachentsev, I. D. 2005, AJ, 129, 178
Karachentsev, I. D., Sharina, M. E., Dolphin, A. E., & Grebel, E. K. 2003a, A&A, 408, 111
Karachentsev, I. D., et al. 2002a, A&A, 385, 21
—. 2002b, A&A, 383, 125
—. 2003b, A&A, 404, 93
—. 2003c, A&A, 398, 467
—. 2003d, A&A, 398, 479
Kniazev, A. Y., Grebel, E. K., Pustilnik, S. A., Pramskij, A. G., Kniazeva, T. F., Prada, F., & Harbeck, D. 2004, AJ, 127, 704
Kormendy, J., & Djorgovski, S. 1989, ARA&A, 27, 235
Kravtsov, A. 2010, Advances in Astronomy, Volume 2010, Article ID 281913
Lisker, T., Glatt, K., Westera, P., & Grebel, E. K. 2006a, AJ, 132, 2432
Lisker, T., Grebel, E. K., & Binggeli, B. 2006b, AJ, 132, 497
—. 2008, AJ, 135, 380
Lisker, T., Grebel, E. K., Binggeli, B., & Glatt, K. 2007, ApJ, 660, 1186
Lotz, J. M., Jonsson, P., Cox, T. J., Croton, D., Primack, J. R., Somerville, R. S., & Stewart, K. 2011, ApJ, 742, 103
Mackey, A. D., et al. 2010, ApJ, 717, L11
Madau, P., Diemand, J., & Kuhlen, M. 2008, ApJ, 679, 1260
Makarova, L. N., et al. 2002, A&A, 396, 473
Malin, D., & Hadley, B. 1999, in Galaxy Dynamics - A Rutgers Symposium, ed. D. R. Merritt, M. Valluri, & J. A. Sellwood, ASP Conf. Ser., 182 (San Francisco, CA: ASP), 445
Martin, N. F., et al. 2009, ApJ, 705, 758
Martínez-Delgado, D., Pohlen, M., Gabany, R. J., Majewski, S. R., Peñarrubia, J., & Palma, C. 2009, ApJ, 692, 955
Martínez-Delgado, D., et al. 2010, AJ, 140, 962
Mateo, M. L. 1998, ARA&A, 36, 435
Materne, J., & Tammann, G. A. 1974, A&A, 35, 441
McConnachie, A. W., et al. 2009, Nature, 461, 66
Miskolczi, A., Bomans, D. J., & Dettmar, R.-J. 2011, A&A, 536, A66
Monaco, L., Saviane, I., Perina, S., Bellazzini, M., Buzzoni, A., Federici, L., Fusi Pecci, F., & Galleti, S. 2009, A&A, 502, L9
Monet, D. G., et al. 2003, AJ, 125, 984
Moore, B., Ghigna, S., Governato, F., Lake, G., Quinn, T., Stadel, J., & Tozzi, P. 1999, ApJ, 524, L19
Mouhcine, M., & Ibata, R. 2009, MNRAS, 399, 737
Mouhcine, M., Ibata, R., & Rejkuba, M. 2010, ApJ, 714, L12
—. 2011, MNRAS, 415, 993
Oemler, Jr., A. 1974, ApJ, 194, 1
Padilla, N. D., et al. 2004, MNRAS, 352, 211
Paturel, G., Petit, C., Prugniel, P., Theureau, G., Rousseau, J., Brouty, M., Dubois, P., & Cambrésy, L. 2003, A&A, 412, 45
Paudel, S., Lisker, T., Kuntschner, H., Grebel, E. K., & Glatt, K. 2010, MNRAS, 405, 800
Peng, E. W., Ford, H. C., Freeman, K. C., & White, R. L. 2002, AJ, 124, 3144
Regan, M. W., et al. 2004, ApJS, 154, 204
Richardson, J. C., et al. 2011, ApJ, 732, 76
Sancisi, R., Fraternali, F., Oosterloo, T., & van der Hulst, T. 2008, A&A Rev., 15, 189

Sandage, A. 1976, AJ, 81, 954
Saviane, I., Held, E. V., & Bertelli, G. 2000, A&A, 355, 56
Schlegel, D. J., Finkbeiner, D. P., & Davis, M. 1998, ApJ, 500, 525
Schweizer, F., & Seitzer, P. 1988, ApJ, 328, 88
Sersic, J. L. 1968, Atlas de galaxias australes
Siegel, M. H., et al. 2007, ApJ, 667, L57
Smith, R. J., Lucey, J. R., Hudson, M. J., Allanson, S. P., Bridges, T. J., Hornschemeier, A. E., Marzke, R. O., & Miller, N. A. 2009, MNRAS, 392, 1265
Szomoru, A., & Guhathakurta, P. 1998, ApJ, 494, L93
Trentham, N., Tully, R. B., & Mahdavi, A. 2006, MNRAS, 369, 1375
Tully, R. B. 1987, ApJ, 321, 280
Tully, R. B., & Fisher, J. R. 1988, Catalog of Nearby Galaxies (Cambridge: Cambridge Univ. Press)
Tully, R. B., & Trentham, N. 2008, AJ, 135, 1488
van den Bergh, S. 1994, AJ, 107, 1328
Walter, F., Brinks, E., de Blok, W. J. G., Bigiel, F., Kennicutt, Jr., R. C., Thornley, M. D., & Leroy, A. 2008, AJ, 136, 2563
Werk, J. K., Putman, M. E., Meurer, G. R., Oey, M. S., Ryan-Weber, E. V., Kennicutt, Jr., R. C., & Freeman, K. C. 2008, ApJ, 678, 888
White, S. D. M., & Frenk, C. S. 1991, ApJ, 379, 52
Williams, M. E. K., et al. 2011, ApJ, 728, 102
Yanny, B., et al. 2003, ApJ, 588, 824
Yun, M. S., Ho, P. T. P., & Lo, K. Y. 1994, Nature, 372, 530
Zucker, D. B., et al. 2004, ApJ, 612, L121
—. 2006, ApJ, 650, L41
—. 2007, ApJ, 659, L21